EFDA–JET–CP(11)01/04

J. Likonen, M. Airila, E. Alves, N. Barradas, S. Brezinsek, J.P. Coad, S. Devaux, M. Groth, S. Grünhagen, A. Hakola, S. Jachmich, S. Koivuranta, T. Makkonen, M. Rubel, J. Strachan, M. Stamp, A. Widdowson
and JET EFDA contributors

Deposition of ^{13}C Tracer in the JET MkII-HD Divertor

Deposition of ^{13}C Tracer in the JET MkII-HD Divertor

J. Likonen[1], M. Airila[1], E. Alves[2], N. Barradas[2], S. Brezinsek[3], J.P. Coad[4], S. Devaux[5], M. Groth[6], S. Grünhagen[4], A. Hakola[1], S. Jachmich[7], S. Koivuranta[1], T. Makkonen[6], M. Rubel[8], J. Strachan[4,9], M. Stamp[4], A. Widdowson[4]
and JET EFDA contributors*

JET-EFDA, Culham Science Centre, OX14 3DB, Abingdon, UK

[1]Association EURATOM-Tekes, Technical Research Centre of Finland, PO Box 1000, FI- 02044 VTT, Finland
[2]Instituto Tecnológico e Nuclear, Sacavém, 2686-953, Portugal
[3]Institute of Energy and Climate Research – Plasma Physics, Forschungszentrum Jülich GmbH, Association EURATOM-FZJ, Partner in the Trilateral Euregio Cluster, D-52425 Jülich, Germany
[4]EURATOM/CCFE Fusion Association, Culham Science Centre, Abingdon, Oxon, OX14 3DB, UK
[5]Max-Planck-Institut für Plasmaphysik, EURATOM Association, 85748 Garching, Germany
[6]Association EURATOM-Tekes, Aalto University, 02015 Espoo, Finland
[7]Laboratory for Plasma Physics, Ecole Royale Militaire/Koninklijke Militaire School, EURATOM-Association "Belgian State", Brussels, Belgium, Partner in the Trilateral Euregio Cluster (TEC)
[8]ALfvén Laboratory, Royal Institute of Technology, Association EURATOM-VR, 100 44 Stockholm, Sweden
[9]Princeton Plasma Physics Laboratory, James Forrestal Campus, Princeton, NJ 08543, New Jersey, USA
** See annex of F. Romanelli et al, "Overview of JET Results", (23rd IAEA Fusion Energy Conference, Daejon, Republic of Korea (2010)).*

Preprint of Paper to be submitted for publication in Proceedings of the
13th International Workshop on Plasma-Facing Materials and Components for Fusion Applications
Rosenheim, Germany
(9th May 2011 - 13th May 2011)

ABSTRACT

Migration of ^{13}C has been investigated at JET by injecting ^{13}C labelled methane at the outer divertor base at the end of the 2009 campaign. The ^{13}C deposition profiles on CFC divertor tiles were measured with secondary ion mass spectrometry and Rutherford backscattering techniques. ^{13}C was mainly deposited near the puffing location on the outer divertor base tiles. High amounts of ^{13}C were also found at the outer vertical target: bottom of the lower and at the top of the upper plates. 33% of the puffed $^{13}CH_4$ was instantly pumped out by the divertor cryopump which is close to the the pump duct entrance. The global ^{13}C transport in the torus was modelled with the EDGE2D/EIRENE and DIVIMP codes and the local ^{13}C migration in the vicinity of the injection location with the ERO code. The DIVIMP and EDGE2D simulations show strong prompt deposition of ^{13}C directly adjacent to the injection point, as well as in the far SOL along both the inner and outer divertor targets. In addition, the measured ^{13}C deposition along the outer divertor wall tiles is qualitatively reproduced. However, EDGE2D and DIVIMP do not predict any deposition along the divertor surfaces facing the private plasma on the inner floor tile and inboard of the outer strike point on Tile 5. The ERO calculations also indicate that majority of the deposition occurs close to the injection location on the vertical face of the LBSRP tile and the horizontal part of Tile 6.

1. INTRODUCTION

Erosion of Plasma Facing Components (PFC) as well as migration of impurities and their subsequent deposition on PFCs have a great impact on the tritium retention and on the lifetime of first wall components in present and future fusion devices. Deposition on JET divertor tiles has been observed to be poloidally non-uniform; i.e. heavy deposition occurs in the SOL at the inner divertor whereas little deposition was measured at the outer divertor [1]. Heavy deposition at the inner divertor has led to flaking on the water-cooled louvres. The transport has been identified by deposition monitors and spectroscopy to be stepwise into the remote areas along the line-of-sight [2,3]. After the DTE1 tritium experiment at JET the majority of retained tritium was observed to reside in the flakes that have spallen from the louvres [1].

Campaign integrated results are, however, difficult to interpret quantitatively because surface analyses are only available after the plasma-facing components have been removed after a campaign during which they have been exposed to a range of different plasma types, geometries and divertor plasma parameters. The deposition at the inner divertor, as analyzed when tiles were removed from the vessel, is the result of typically two years of JET operations with about 3000 - 4000 discharges covering many types of plasma operation [4,5]. It is thus difficult to conclude which aspects of operation are important in controlling the deposition. In order to gain better understanding of impurity migration the long-term post-mortem surface analyses have to be supplemented e.g. by tracer experiments in which small quantities of a marker gas are injected into successive, similar plasma discharges at the end of an experimental campaign. The tracer injection experiments are suitable for trace impurity simulations to elucidate the transport processes.

This paper focuses on the 2009 experiment in JET with carbon wall. Marker gas, ^{13}C labelled methane, was puffed toroidally symmetrically through 24 injection locations into the outer scrape-off layer of H-mode plasma in deuterium with the Outer Strike Point (OSP) on the Load Bearing Septum RePlacement (LBSRP) tile. Though toroidally symmetric, the injection was inhomogeneous due to the fact that the injection was only through one out of every four outer base tiles 6, that comprise one of the 24 divertor modules. The injection was thus toroidally periodic. Here we report the results of post-mortem surface analyses obtained using Secondary Ion Mass Spectrometry (SIMS) and Rutherford BackScattering (RBS). The results of the 2009 experiment are compared with the results from the previous puffing experiments. In addition, the ^{13}C transport is modelled with the DIVIMP, EDGE2D/EIRENE and ERO codes.

2. EXPERIMENTAL SETUP AND DEPOSITION MEASUREMENT TECHNIQUES

In JET, tracer injections have been carried out in 2001 [6,7], 2004 [8], 2007 [9] and 2009 by puffing isotopically labelled methane ($^{13}CH_4$) repeatedly into the torus during the last operational day before a major shutdown. The main parameters for the ^{13}C puffing experiments are given in Table 1. In the 2001 and 2007 experiments, $^{13}CH_4$ was puffed from the main chamber, whereas in 2004 and 2009 the injection was made from the divertor. In 2001 ohmic discharges were used while in all the other experiments the plasma was of ELMy H-mode type. Figure 1 shows the locations of ^{13}C injection in each experiment, and the geometry of the divertor tiles and separatrix in 2009, although there will be a discussion on the actual OSP position later. In 2001, $^{13}CH_4$ was injected through a gas introduction module at the top of the vessel (GIM 5) during 13 ohmic pulses [6]. In 2004, the puffing experiment was performed through 48 toroidally symmetric nozzles (GIM10) from the outer divertor wall between Tiles 7 and 8 [8]. In the 2007 experiment $^{13}CH_4$ was injected from near the lower hybrid antenna (GIM 6). GIM6 consists of a pipe with 8 puffing holes located in a single toroidal but different poloidal positions.

During the final experimental day of the JET campaign in 2009, 30 identical discharges (Pulse No's: 79816 – 79853) were run with $^{13}CH_4$ injection from the outer divertor base tile. The total injected amount of ^{13}C was 7.12 g (3.30×10^{23} particles). The discharges were 2.5 T, 2.5 MA H-mode shots in deuterium with a line-averaged density of 14.8×10^{19} m^{-2} and an auxiliary heating power of 15 MW. The ELMs were of type I having an average core energy loss of about 400 kJ. The strike points were on the lower inner vertical target plate (Tile 3) and on the LBSRP (Tile 5). The average ^{13}C puffing rate was 2.5×10^{21} atoms/s.

The global gas balance over the ^{13}C experiment was measured by regenerating the cryopump before the first plasma, and then after the experiment regenerating the cryopump again and collecting the gas for analysis of its content and composition [10]. During the first step of the pump regeneration the cryogenic panels were warmed up gradually from liquid helium temperature (LHe, 4 K) to liquid nitrogen temperature (LN_2, 77 K) and a total amount of 25.3 barl gas was collected through the Active Gas Handling System (AGHS) mechanical forevacuum system. The regenerated

gas was analysed using gas chromatography (GC) [11].

The tiles were analysed with the RBS and secondary ion mass spectrometry (SIMS) techniques. At the University of Sussex, RBS measurements were carried out using a 2.5-MeV H^+ beam from the Van de Graaff accelerator [12]. At ITN in Portugal, the amount of ^{13}C deposited on Tiles 6 was determined at a scattering angle of 145^o by means of Enhanced Proton Scattering (EPS) near the resonance energies for ^{13}C in the energy range of 1.5 – 1.8 MeV. The RBS and EPS spectra were simulated using the SIMNRA [13] and WiNDF [14] programs. The SIMS depth profiles of the tiles from one toroidal location were taken at several poloidal positions of the analysed samples. SIMS analyses of the samples were made with a double focusing magnetic sector instrument (VG Ionex IX-70S) at Technical Research Centre of Finland using a 5 keV O_2^+ primary ion beam with a current of 500 nA [7]. Calibration samples were measured separately with Time-Of-Flight Elastic Recoil Detection Analysis (TOF-ERDA) at the University of Helsinki.

3. EXPERIMENTAL RESULTS

A total amount of 25.3 barl gas was collected by AGHS and analysed with GC. It cannot separate ^{13}C from ^{12}C so it was assumed that all carbon is ^{13}C. This assumption is reasonable because usually the amount of CH_4 is below 1% indicating that the high amount of CH_4 detected must be due to the $^{13}CH_4$ puffing. The amount of CH_4 in the analysed gas was 15.7% and that of $C_2H_4 + C_2H_6$ 0.22%, so the amount of ^{13}C in $^{13}CH_4$ was 1.07×10^{23} and in $^{13}C_2H_4 + {}^{13}C_2H_6$ 0.032×10^{23} atoms, respectively. The background level of the C_2H_x species was below 0.1%. The total amount of puffed ^{13}C was 3.3×10^{23} atoms. Thus, the AGHS results indicate that about 1/3 of the puffed ^{13}C was directly pumped away and will not be present in the post-mortem surface analyses. Direct pumping of ^{13}C is the main mechanism because the amount of other hydrocarbons in the analysed gas was very small.
Table 1 shows the amount of deposited ^{13}C in different areas of the vessel. In 2001, most of the ^{13}C was found at the inner divertor whereas the deposition pattern is more balanced in 2004, 2007 and 2009. This is most likely due to longer migration path in the SOL for the 2004, 2007 and 2009 experiments so less ^{13}C was migrating towards the inner divertor and more towards the outer divertor. The amount of ^{13}C at the outer divertor in 2009 is an underestimation because not all the surface analysis results have yet been evaluated.

Figures 2-4 show the normalised surface density of ^{13}C (deposited $^{13}C/cm^2$/injected ^{13}C) as a function of the poloidal distance around the divertor. About 8.8% was found on the base tiles, 1.6% on the inner target, and 4% on the outer target. The highest ^{13}C concentrations were found near the puffing location on Tile 6, but also high amounts of ^{13}C on Tile 5 in the region between the outer strike point (OSP) and the puffing location, as well as at the bottom of Tile 7 and at the top of Tile 8 were observed.

On Tile 1, the ^{13}C amount was higher in the 2001 and 2007 experiments than in 2004. In 2009, the ^{13}C amount was the lowest. This could be due to a longer migration path along the SOL in the 2004 and in 2009 experiments since puffing was carried out from the divertor, whereas in the

2001 and 2007 experiments the gas injection was made in the main chamber. Moreover, EDGE2D simulations have indicated that main deposition mechanism above the Inner Strike Point (ISP) at the inner divertor is migration through the main SOL via the top of the vessel from the outboard to the inboard side[7]. Experimental measurements using fast reciprocating probe [15] have shown that such SOL flows occur from the low field to the high field side. On Tile 3, the ^{13}C distributions for the 2007 and 2009 experiments are similar: there is a peak in the ^{13}C distribution above the ISP at x ~ 350 mm and a minimum below the ISP, respectively (see Fig.2). A similar peak is also observed for ^{13}C in the 2001 experiment, although it is located ~ 30mm higher on Tile 3. The ^{13}C distribution in 2004 is different from the other ones: there is a dip at x ~ 350mm where the 2007 and 2009 distributions have a peak. This is not related to the location of the ISP because in 2004 and 2009 the positions of the ISP were the same, whereas in 2007 the ISP was ~40 mm lower than in 2009. Moreover, the 2004 distribution increases as a function of the x coordinate (for x > 350nm) whereas the 2007 and 2009 ones decrease. The deposit on Tile 3 below the ISP is thought to be due to the $\boldsymbol{E}\times\boldsymbol{B}$ drift of ^{13}C ions from the OSP through the Private Flux Region (PFR) to the ISP from where it is subsequently eroded due to ELMs. The main difference between the 2001, 2007 and 2009 experiments, apart from the injection location, is that in 2001 ^{13}C was injected into L-mode plasmas and in 2007 and 2009 into H-mode plasmas. Correspondingly, the 2007-2009 experiments had different SOL transport properties (e.g. higher particle and heat fluxes), an H-mode pedestal, and ELMs.

The divertor floor (Tiles 4-6) was in the PFR in all the ^{13}C puffing experiments except in 2009 when the OSP was on Tile 5 (see Fig. 1 for the 2009 geometry). In 2001, only a few samples from the divertor floor tiles were analysed so comparison with the other experiments is not possible. The overall deposition pattern on the floor tiles for all the ^{13}C puffing experiments is quite similar (see Fig. 3). For the 2004 case, the ^{13}C amount is approximately constant on the horizontal part of Tile 4 and decreases towards the sloping part of Tile 4. In contrast, the ^{13}C deposition pattern in 2007 has a maximum on the sloping part of Tile 4 and the ^{13}C amount on the horizontal part is smaller. In 2009, the ^{13}C amount on the horizontal part is relatively constant and it is smaller than in 2004. This will be discussed later. The main deposition mechanism on Tile 4 is assumed to be the emission of ^{13}C from the ISP.

The ^{13}C concentration on the inboard part of Tile 5 in 2009 is very low (1.5×10^{-8} or less). However, there is a distinct increase in the concentration with the major radius and is maximum at the outboard edge of the tile. In 2004, the ^{13}C distribution has, however, a hollow profile with maxima at both ends of the tile. The ^{13}C amounts on Tile 5 in 2007 and 2009 are comparable except near the outboard edge of the tile where the ^{13}C distribution in 2009 has a distinct peak. This peak is due to migration of ^{13}C from the puffing location on Tile 6 and due to the walking process which will be explained later.

On Tile 6, the ^{13}C distribution has a peak on the horizontal part of the tile both in 2004 and 2007. The distribution in 2009 shows a heavy periodic toroidal ^{13}C deposition band near each puffing hole on Tiles 6 and the ^{13}C amount is much higher than in the previous experiments since

the puffing was made through 24 puffing holes in Tiles 6. ^{13}C has also migrated to the sloping part and the shadowed area of Tile 6, and the amount is higher in 2009 than in 2004 and 2007.

The normalised 2009 ^{13}C deposition pattern on the outer divertor has a maximum of ~4×10^{6} both at the bottom of Tile 7 and at the top of Tile 8, with similar values as those in previous experiments. On Tile 7 the concentration of ^{13}C falls exponentially by two orders of magnitude from the bottom to the centre of the tile, then there is a approximately constant level with increasing x coordinate before increasing again over the upper part of Tile 8. The patterns on Tile 8 in 2007 and 2009 were similar which is mainly due to the angle between the field lines and the surface of Tile 8. In this region, the tile surface is shielded from the main chamber by intersecting Tile 8 near the top edge. The dip at the bottom of Tile 8 is due to the shadowing caused by the field lines intersecting the top of Tile 8.However, the maximum on Tile 7 clearly relates to the OSP position, so in 2009 is at the bottom of the tile whilst in 2007 and 2004 were at the centre and near the top of the tile, respectively. The ^{13}C distribution has a local minimum near the OSP (x ~ 1320mm in 2007 and x ~ 1400 mm in 2004) which is attributed to re-erosion [7]. The 2004 distribution has also a peak in the shadowed area near the top of the tile just below the puffing location. This peak is attributed to local deposition near the opening of the gas inlet system.

A toroidal ^{13}C deposition band near each 24 puffing holes was observed on Tiles 6. Figure 5 shows a 2D map of ^{13}C distribution. The highest ^{13}C amounts were found at the same toroidal location just outboard from the puffing hole (indicated by the white circle on the figure). The poloidal coordinate is the distance radially outwards from the inboard edge of Tile 6. The entire deposition band is more or less completely shadowed by Tile 5. The deposit is probably caused by neutral radicals that have had some dissociation when they left the puffing hole and encountered the plasma edge at the shadow boundary. The neutral radicals created at the plasma boundary can have some chance of going back into the shadow and can stick to that surface. It is unlikely to be pure methane since these will not stick to the surface of Tile 6.

4. MODELLING TOOLS AND SETUP FOR THE ^{13}C EXPERIMENTS IN 2009

Modelling of global migration of ^{13}C in JET injection experiments has been done using the DIVIMP and EDGE2/EIRENE codes. The DIVIMP [16] simulations of the ^{13}C transport and deposition were carried out on deuterium plasmas calculated with DIVIMP's own onion-skin solver (OSM) [17], utilising the measured ion fluxes and electron temperatures along the outer plate as boundary conditions. Due to lack of Langmuir probe measurements along the inner plate, the outer plate profiles were duplicated for the inner plate as well. Upstream from the plates, and on a two-dimensional grid, the plasma conditions for electron temperature and density, ion temperature, electric potential, and plasma flow were calculated using the fluid conservation equations for particles, momentum, and energy. In lieu of methane, ^{13}C neutrals (of the order 100000 particles) were injected at the location corresponding to the actual gas injection module; the break-up chain of methane was not followed in these studies. The carbon neutrals may randomly walk within

the divertor plasma, and ionize given plasma temperature and density, as calculated from the ADAS rate coefficients. The trajectory of ^{13}C ions was subsequently followed both in the direction parallel to B using a force balance equation [18], and perpendicular to B assuming radially constant diffusion coeffiecient. Only prompt deposition was considered; re-erosion and subsequent re-deposition of ^{13}C has not yet been studied with DIVIMP. The total predicted ^{13}C deposition was finally normalised to the total injected ^{13}C amount.

The EDGE2D/EIRENE code was applied as described in Ref [7]. The carbon ionization near the injector and ion transport to the divertor was modelled. The code assumes toroidal symmetry and thus the actual ^{13}C source is treated toroidally symmetric. The methane injection rate is large, but the code treated the injection as atomic carbon. The carbon injection and its perturbation to the local SOL were toroidally averaged while the hydrogen perturbation was ignored. The carbon neutrals were followed by the Monte Carlo code EIRENE. The ELMs were not treated explicitly since in Ref. [7] it was found that there was little long-range migration associated with the ELM itself.

Local migration, deposition and erosion were simulated with the 3D Monte Carlo impurity transport code ERO [19,20]. The simulation was set up by defining a rectangular simulation volume tilted by 45^{o} to obtain maximal coverage of Tiles 5 and 6 next to the injection location (see Fig. 1). For technical reasons Tile 7 was left outside the volume, but the test particle trajectories through the top edge of the box can be extrapolated to Tile 7 to obtain an estimate of deposition there. The simulation domain is about 23 cm along the divertor, 11cm thick and 73cm long toroidally, corresponding to one toroidal period of the injection configuration. Periodic boundary conditions were applied in the toroidal direction to account for the effect of neighbouring injectors. ERO modelling focuses on a reference case that used the following parameters: Reflection of ions was calculated according to TRIM data, whereas for hydrocarbons an effective sticking coefficient S = 0.1 was used. It was assumed that the erosion of deposited (soft hydrocarbon) layers is enhanced by a factor of 5 compared to the substrate (graphite). A uniform plasma background was used with $n_e = 5 \times 10^{18}$ m^{-3}, $T_e = T_i = 5eV$ and the flow velocity calculated assuming M = 1. A plasma-shadowed region (very low temperature and density) was defined in front of the injection as implied by the magnetic geometry. ELMs were not taken into account in the calculations. Several parameters including density, temperature, enhanced re-erosion, velocity direction of injected molecules, perpendicular diffusion coefficient, Mach number assumption and shadow model were varied. The deposition pattern and locally deposited fraction were rather robust with respect to these variations and in the following we only refer to results obtained in the reference case.

5. MODELLING RESULTS

Simulation of the ^{13}C injection from the outer divertor gas module (GIM9) with the DIVIMP code shows strong prompt deposition of ^{13}C directly in the vicinity of the injection point, as well as in the far SOL along both the inner and outer divertor targets (see Fig. 6). A scan of the cross-field diffusion coefficient with D = 0.5, 1 and 2 m^2/s was made and the results for the deposition profiles

are shown in Figure 6. Deposition at the inner divertor decreases as a function of D, but increases at the outer divertor. Near the puffing location the diffusion coefficient has a minor effect as can be seen in Fig.6. The deposition at the injection location on Tile 6 is about an order of magnitude higher than the measured values, while the DIVIMP simulations qualitatively reproduce the measured ^{13}C deposition near the top of Tile 7 and bottom of Tile 8, but not at the bottom of Tile 7 and top of Tile 8. However, the code does not predict any deposition along the divertor surfaces facing the private plasma (Tiles 4 and inboard of the OSP on Tile 5) because the ***ExB*** drifts are not included in DIVIMP. In addition, re-erosion phenomena were not taken into account in the simulations. The strong deposition near the injection location indicates prompt re-deposition of carbon ions upon their ionisation close to the outer plate, whereas the deposition along Tiles 1 and 8 suggests ion transport away from the plates, radial outward diffusion, and flow of ^{13}C ions toward the plates in the far SOL. The simulations suggest that long-range transport of ^{13}C ions from the outer divertor across the SOL to the inner divertor leg occurs, subsequently leading to deposition on Tile 1.

The EDGE2D results indicate that 88 to 98% of the injected ^{13}C is redeposited in the vicinity of the injector (see Fig.7). Only 10^{-3} to 10^{-4} of the injected ^{13}C leaves the outer divertor for the main chamber SOL and eventually is deposited in the inner SOL near the inner target. A scan was made with separate EDGE2D/EIRENE runs for cases with carbon SOL diffusion coefficient of 0.1, 1 and 2 m^2/s. The outer target deposits were little influenced by the diffusion with predicted deposits about 100 times larger than experimentally observed. Re-erosion by hydrogen ion bombardment would reduce the C deposit to experimental values but re-erosion phenomena were not included in the calculations. Correspondingly, the deposit near Tile 1 is predicted by EDGE2D/EIRENE to be about 20 times smaller than was observed. Similarly, these deposits would be enhanced by the re-erosion at the outer target.

Figure 8 (a) shows the deposition pattern obtained with ERO. About 37% of the injected ^{13}C is deposited within the simulation volume, whereas 59% is lost (mostly as neutrals) towards the outer divertor and 4% towards the X-point. In the experiment, about 16% of the injected ^{13}C was deposited inside the ERO simulation volume. A clear majority of the deposition occurs close to the injection location (on the outer end face of Tile 5 and the horizontal part of Tile 6), the deposition tail extending about 50 cm. This indicates that the local deposition is dominated by ions. The measurements show that there is significant deposition also on the sloping part of Tile 5 (see Fig.8 (b)), which is not explained by the present simulations – not even by the parameter variations with significantly lower density or temperature that allow longer cross-field transport paths of the source particles before ionization. A possible explanation could be an erosion source of deposited ^{13}C near the OSP due to ELMs.

The neutrals lost from ERO simulation towards the outer divertor were traced in a post-processor, giving their first-hit distribution on Tile 7 (Fig.8 (c)) but neglecting reflection and re-erosion. Therefore the obtained profile is a definite upper limit for the deposition originating directly from the injection source. The rather steeply decreasing pattern is explained by the fact

that the velocity distribution of escaping neutrals has a strong component to +z direction that is efficiently shadowed in the upper part of the curved Tile 7.

DISCUSSION

Three factors can account for the deposition on the inner divertor. Firstly, erosion rates are larger on the outer target due to higher energies of impinging deuterons and therefore it is improbable that deposits will be formed there [21]. Secondly, thermal forces are larger near the outer, when compared with the inner, divertor entrance inhibiting parallel motion of carbon to this target [22]. Thirdly, at the machine top the experimentally measured SOL flow is directed towards the inner target [21].

In 2001, ohmic discharges without ELMs were used in the puffing experiment, but in all the other experiments ELMs were present. The principal difference in the results shown in Figure 2 is that the amount of ^{13}C on Tile 1 is higher for the main chamber puffing experiments than for those with puffing at the divertor. The deposits far from the ISP (or on Tile 1) were similar between 2001 and 2007, but the deposit in the vicinity of the ISP was 5 to 10 times lower for all the discharges with ELMs (including the 2004 and 2009 experiments). Plausibly, the ELMs increase re-erosion of ^{13}C deposits near the ISP as observed in-situ for normal deposits by deposition monitors [23] and spectroscopy [3]. EDGE2D did not attempt to model these re-erosion effects due to ELMs in the case of the 2009 experiment. In the 2004 experiment, the ^{13}C migration to the ISP from the OSP was explained by $\boldsymbol{E}\times\boldsymbol{B}$ drifts in the PFR. The $\boldsymbol{E}\times\boldsymbol{B}$ drift was included in the other experiments as well, but it is less important for the main chamber injection made in 2007 than for the divertor injections. This is because the OSP acts as source for the $\boldsymbol{E}\times\boldsymbol{B}$ drift and there is less ^{13}C reaching the OSP. The 2009 and the previous experiments plausibly also have contributions from multiple ^{13}C re-erosion and redeposition short range steps (called walking [8]) towards the ISP from deposits further up on Tile 3.

In the PFR, the ^{13}C was assumed to transport as neutrals created at the strike points as was modelled in Ref [3]. The C neutral emission from the strike point was not calculated [7] and the magnitude was used as a free parameter. The emission from the strike point was assumed isotropic to explain the observed ^{13}C deposits. This is different from what is normally assumed ($\cos\theta$- or $\cos^2(\theta)$-like distribution with respect to the surface angle) for the emission of physically sputtered material from a surface. The 2009 deposits could not be explained by $\cos\theta$- or $\cos^2(\theta)$-like ^{13}C emission from the strike points [7]. Re-erosion inside the PFR (potentially caused by hydrogen neutrals) may have altered the $\cos\theta$-like deposits to somehow look like isotropic deposits but the measurements provide no direct evidence for this. Since re-erosion in the PFR [24,25] has not been considered here, such possibilities as well as other physical processes (e.g. molecular dissociation effects), cannot be excluded, however.

Smaller deposition on the horizontal part of Tile 4 in 2009 than in 2004 is an indication of lower re-erosion from the ISP and thus less arriving from the OSP. As explained earlier the ^{13}C migration

from the OSP to the ISP is due to $\boldsymbol{E}\times\boldsymbol{B}$ drifts. Furthermore, the multi-step walking mechanism was proposed to explain the ^{13}C migration along the outer divertor towards the OSP in the 2004 experiment allowing ^{13}C finally to cross into the PFR. However, in 2009 the OSP was located on Tile 5 and due to the magnetic configuration the "walking" occurs now away from the OSP. This difference in the walking is another possible reason for smaller deposition on the horizontal part of Tile 4 and on the PFR side of Tile 5 in 2009 than in 2004. The modelling for 2009 predicts no ^{13}C on the PFR side of the OSP, whereas as mentioned in the Experimental results and shown in Figure 3 there appears to be a significant amount inboard from the marked OSP (which is obtained from magnetic data). By comparing with Infra-Red spectroscopy (IR) data it is believed that the marked OSP actually indicates the point of maximum flux during ELMs and not the correct strike point (which should refer to the inter-ELM period). Data currently being evaluated suggests the difference can be as much as 40 mm, which would mean the ^{13}C deposition is at, rather than inboard of, the OSP for the inter-ELM, and thus modelled period.

Tile 6 shows similar deposition both in 2004 and 2007 (see Fig.3) which means that conversion to neutrals at the OSP and deposition in the PFR had about an equal probability both in 2004 and 2007. In 2009, the deposition on Tile 6 is different due to the heavy toroidal deposition band caused by the puffing through a hole in Tile 6. In addition, the walking mechanism away from the OSP may increase the ^{13}C migration towards the sloping part of Tile 6.

Future studies with DIVIMP will assess the uncertainty in the predictions due to the assumed (measured) plasma conditions at the outer plate, and investigate the effect of lower temperatures and higher densities at the inner plate. The efficiency of transport of ^{13}C in the parallel-B direction as well as across the PRF will be assessed by varying the perpendicular diffusion coefficient. Furthermore, DIVIMP ^{13}C simulations will be carried out for comparison with background provided by EDGE2D/EIRENE (including deuterium and ^{12}C), and also be compared to EDGE2D/EIRENE predictions simulating ^{13}C injection. In the case of EDGE2D the simulations in this paper were made using a grid which does not extend to the outer divertor target tiles. An updated grid exists now that extends closer to the outer divertor target tiles. Re-erosion phenomena were neglected which resulted in too high ^{13}C amounts near the injection location and at the outer divertor while too little deposition occurred at the inner divertor. These re-erosion phenomena and the extended grid will be included in future EDGE2D calculations.

In the ERO modelling the reference case can approximately reproduce the level of deposition in the vicinity of the injection (also outside the simulation domain on Tile 7), but it is evident from the results that global migration can create important secondary ^{13}C sources (such as erosion in the inner divertor) that are neglected in ERO. Consequently the modelling underestimates significantly the deposition in certain locations (e.g. slope of Tile 5). In further modelling the most important development will be replacing the present uniform plasma backgrounds used in ERO with realistic plasma backgrounds from EDGE2D or OSM. This makes it possible to include also drifts that have been shown to be important for local ^{13}C migration in ASDEX Upgrade [26].

CONCLUSIONS

Migration and deposition of ^{13}C at JET with carbon based PFC were investigated by injecting $^{13}CH_4$ into the torus from the outer divertor base through 24 holes in Tiles 6 (GIM 9) at the end of the 2009 experimental campaign. The surface density of ^{13}C was determined from a full poloidal set of divertor tiles using SIMS and RBS techniques. The highest ^{13}C amounts were found near the puffing location on Tile 6, where a strong toroidal deposition band was observed. In addition, there was a high amount of ^{13}C near the bottom of Tile 7 and at the top of Tile 8. The amount of ^{13}C on the inner divertor tiles was clearly smaller than on the outer divertor tiles. The cryo-panels of the divertor cryogenic pump were regenerated before and after the ^{13}C puffing experiment, and the released gas was pumped and analysed by the AGHS. The GC results indicate that about 1/3 of the puffed ^{13}C was instantly pumped away and cannot be found in the post-mortem surface analyses.
The DIVIMP, EDGE2D/EIRENE and ERO codes were used for modelling the 2009 experiment. The ^{13}C deposits along the inner divertor tiles on the SOL side of the ISP arrive at the inner divertor leg from the main chamber SOL. The deposits in the PFR are likely due to neutrals originating at the ISP. These deposits are probably also subject to further erosion from deuterium neutrals that originate at the ISP. Walking along Tile 5 occurs away from the OSP which is different from the 2004 and 2007 experiments where walking occurred along the outer divertor Tile 7 towards the OSP.

The DIVIMP and EDGE2D calculations show strong prompt deposition of ^{13}C directly close to the injection point, as well as both at the inner and outer divertor. The DIVIMP simulations qualitatively reproduce the measured ^{13}C deposition along outer divertor Tile 8, which increased with distance from the injection location and the OSP. However, DIVIMP and EDGE2D do not predict any deposition along Tile 4 and inboard of the OSP on Tile 5.

The ERO calculations show that about 37% of the injected ^{13}C is deposited within the simulation volume, whereas 59% is lost (mostly as neutrals) towards the outer divertor and 4 % towards the X-point. These numbers ignore the pumped out amount of ^{13}C. A clear majority of the deposition occurs close to the injection location on the vertical face of Tile 5 and the horizontal part of Tile 6. The measurements show that there is significant deposition also on the sloping part of Tile 5. The neutrals lost from the ERO simulation towards the outer divertor were traced in a post-processor, giving their first-hit distribution on Tile 7. The obtained profile is a definite upper limit for the deposition originating directly from the injection source because reflection and re-erosion effects were neglected.

ACKNOWLEDGEMENTS

This work, supported by the European Communities under the contract of Association between EURATOM/Tekes, was carried out within the framework of the European Fusion Development Agreement. The views and opinions expressed herein do not necessarily reflect those of the European Commission.

REFERENCES

[1]. Coad J.P. et al 2001 Journal Nuclear Materials **290–293** 224
[2]. Esser H.G. et al 2005 Journal Nuclear Materials **337-339** 84
[3]. Brezinsek S. et al 2005 Journal Nuclear Materials **337-339** 1058
[4]. Widdowson A.M. et al 2009 Physica Scripta **T138** 014005
[5]. Coad J.P. et al these proceedings
[6]. Likonen J. et al 2003 Fusion Engineering and Design **66–68** 219
[7]. Strachan J.D. et al 2004 Proc. 30th EPS Conf. on Controlled Fusion and Plasma Physics London, UK, vol. 28G (ECA) P-1.136
[8]. Strachan J.D. et al 2008 Nuclear Fusion **48** 105002
[9]. Likonen J. et al 2011 Journal Nuclear Materials at press
[10]. Brezinsek S. et al 2011 Journal Nuclear Materials at press
[11]. Grünhagen S. et al 2010 Fusion Science and Technology, at press
[12]. Coad J.P. et al 2006 Nuclear Fusion **46** 350
[13]. Mayer M., SIMNRA User's Guide, Report IPP 9/113, Max-Planck-Institut für Plasmaphysik, Garching, Germany, 1997
[14]. Jeynes C. et al 2003 Journal of Physics D: Applied Physics **36** R97-R126
[15]. Erents S.K. et al 2000 Plasma Physica and Controlled Fusion 42 905
[16]. Stangeby P. et al 1988 Nuclear Fusion **28** 1945
[17]. Stangeby P. et al Journal Nuclear Materials 2003 **313–316** 883
[18]. Neuhauser J. et al 1984 Nuclear Fusion **24** 39
[19]. Kirschner A. et al 2000 Nuclear Fusion **40** 989
[20]. Airila M.I. et al to be submitted to Nuclear Fusion
[21]. Pitts R.A. et al 2005 Journal Nuclear Materials **337-339** 146
[22]. Strachan J. et al 2004 Nuclear Fusion **44** 772
[23]. Kreter A. et al 2009 Physical Review Letters **102** 045007
[24]. Airila M.I. et al 2011 Journal Nuclear Materials at press
[25]. Esser H.G. et al 2009 Journal Nuclear Materials **390-391** 148
[26]. Aho-Mantila et al 2011 Journal Nuclear Materials at press

Campaign	Discharges	B_t (T)	I_p (MA)	n_e ($\times 10^{19}$ m^{-2})	P_{aux} (MW)	^{13}C injection ($\times 10^{23}$ atoms)
2001	54330 - 54345	2.5	2.4	7.5	-	1.3
2004	63405 - 63445	2.4	1.2	7.8	4.7	4.3
2007	70729 - 70749	1.6	1.6	10.8	9	9.3
2009	79816 - 79853	2.5	2.5	14.8	15	3.3

Table 1: Main parameters of the different ^{13}C puffing experiments.

	2001	2004		2007	2009
Inner div.	45	3.2	2.9	7.7	1.6
Floor	0.9	6.3	7.5	5.6	8.8
Outer div.	0.4	17	16.4	5.5	4
Main wall	n/a	n/a	2.7	4.1	0.4
Pumped amount	n/a	n/a	n/a	n/a	33
Total	46.3	26.5	29.5	22.9	14.8

Table 2: Deposition of ^{13}C in different areas of the vessel during the puffing experiments.

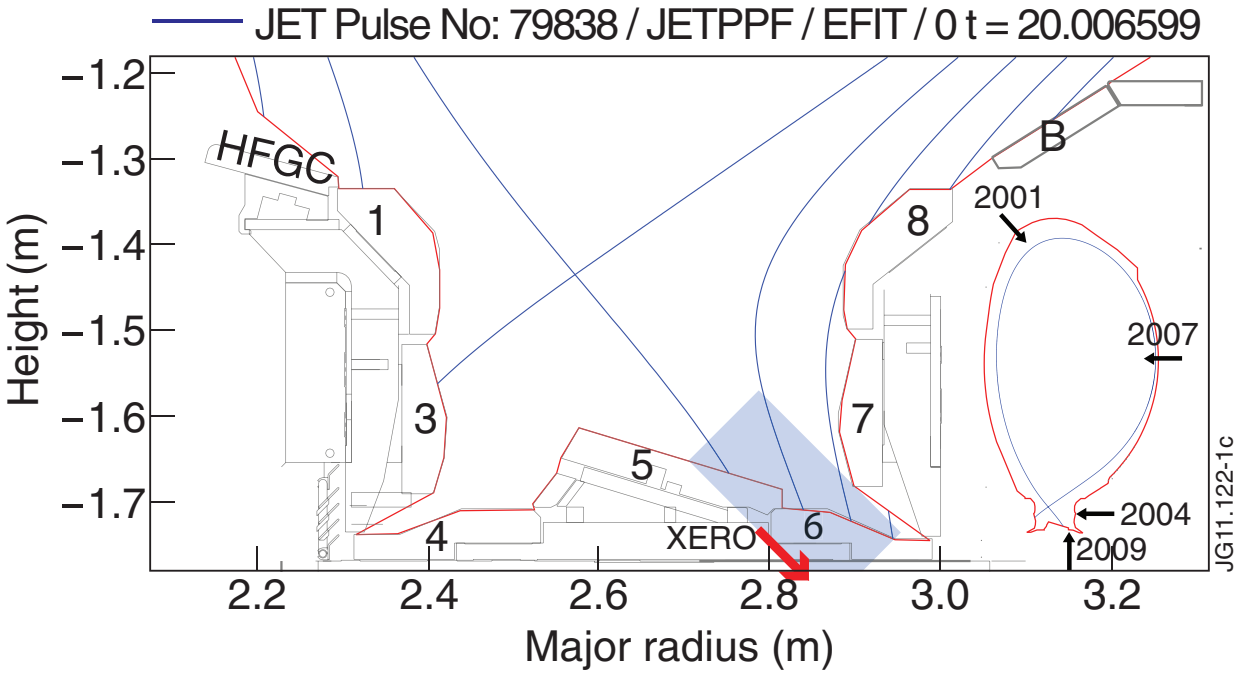

Figure 1: The geometry of JET divertor tiles (MkII-HD) in 2009. Magnetic configuration used in the ^{13}C puffing experiment is also shown. The insert shows the puffing locations for the 2001, 2004, 2007 and 2009 experiments, and the blue box the simulation volume used in the ERO calculations. X_{ERO} and red arrow indicate the x coordinate used in the ERO simulations.

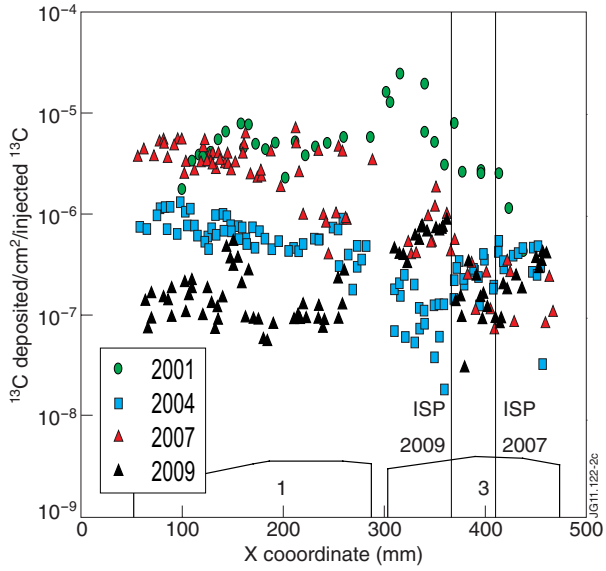

Figure 2: Experimental and normalised ^{13}C distribution on Tiles 1 and 3 for the 2001, 2004, 2007 and 2009 experiments. ISP shows the location of the inner strike point for the 2007 and 2009 experiments. The origin of the x coordinate is on the left-hand side of the High Field Gap Side (HFGS) tile. At the inner divertor it goes along the vertical axis, on the floor along the major radius, and at the outer divertor along the vertical axis.

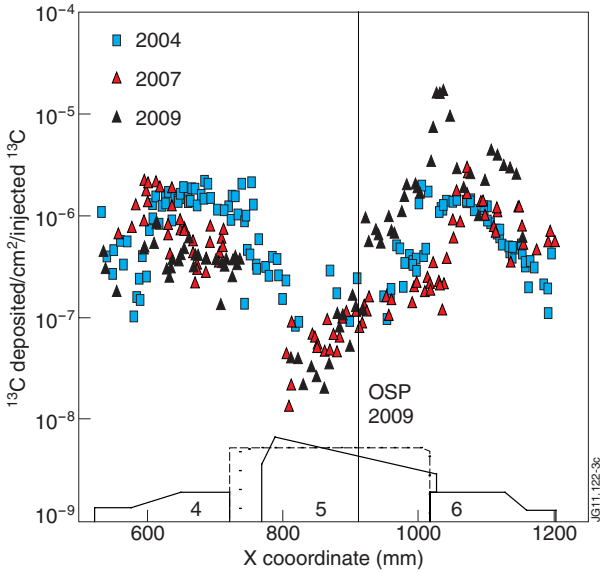

Figure 3: Experimental and normalised ^{13}C distribution on Tiles 4, 5 and 6 for the 2004, 2007 and 2009 experiments. Dashed line shows the profile for Tile 5 in 2004. OSP shows the location of the outer strike point in 2009.

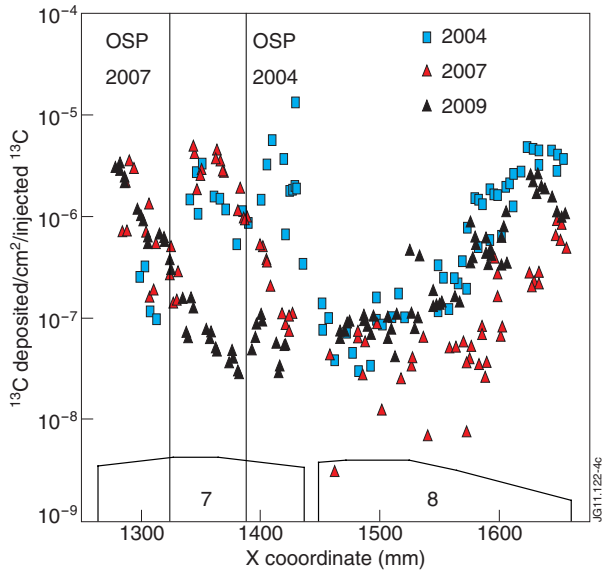

Figure 4: Experimental and normalised ^{13}C distribution on Tiles 7 and 8 for the 2004, 2007 and 2009 experiments. OSP shows the location of the outer strike point for the 2004 and 2007 experiments.

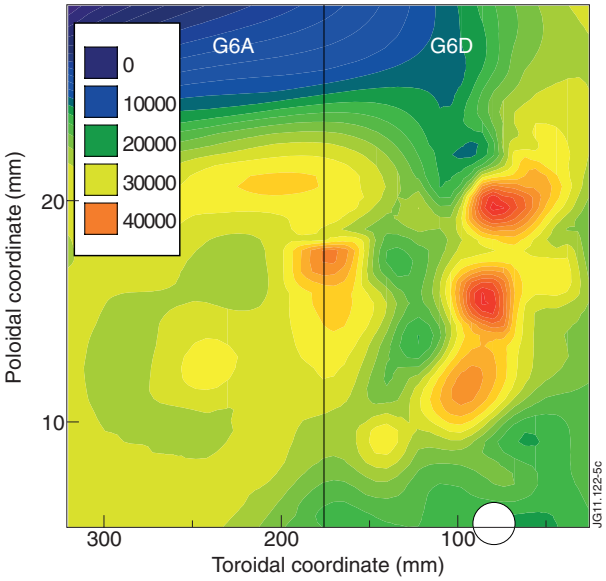

Figure 5: 2D map for ^{13}C on Tiles 6A and 6D. The ^{13}C amounts are in units of 10^{15} cm^{-2}. The location of the puffing hole in Tile 6D is indicated with a white circle.

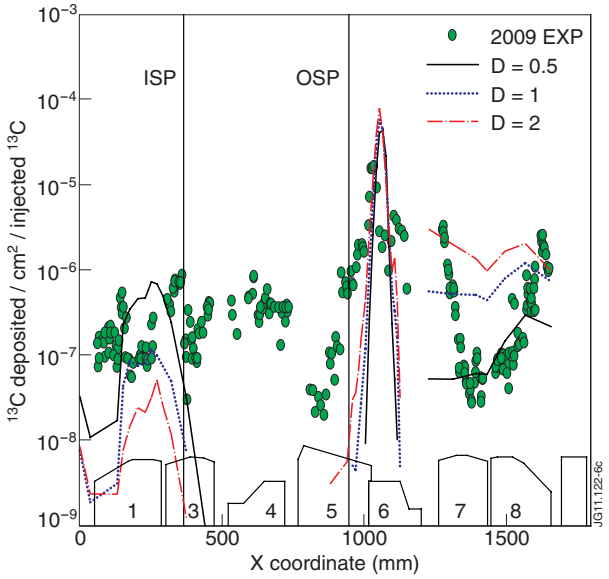

Figure 6. ^{13}C deposition profiles calculated with the DIVIMP code. Calculations were made using a cross-field diffusion coefficient of D = 0.5, 1 and 2 m^2/s. Green circles are the experimental results of the 2009 experiment.

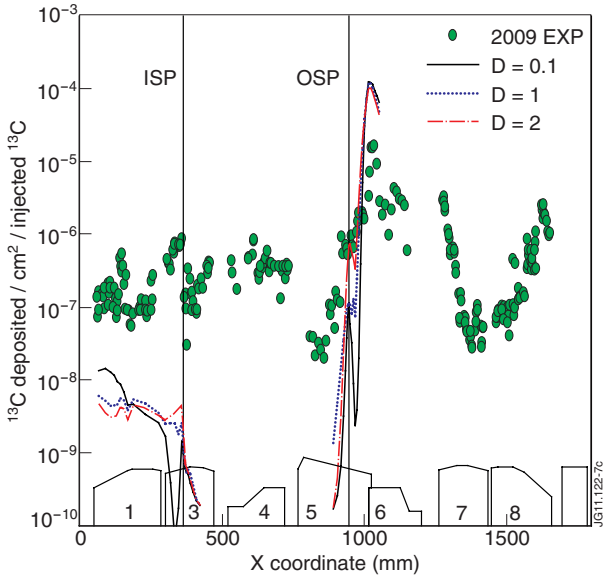

Figure 7. ^{13}C deposition profiles calculated with the EDGE2D code. Calculations were made using a cross-field diffusion coefficient of D = 0.1, 1 and 2 m^2/s. Green circles are the experimental results for the 2009 experiment.

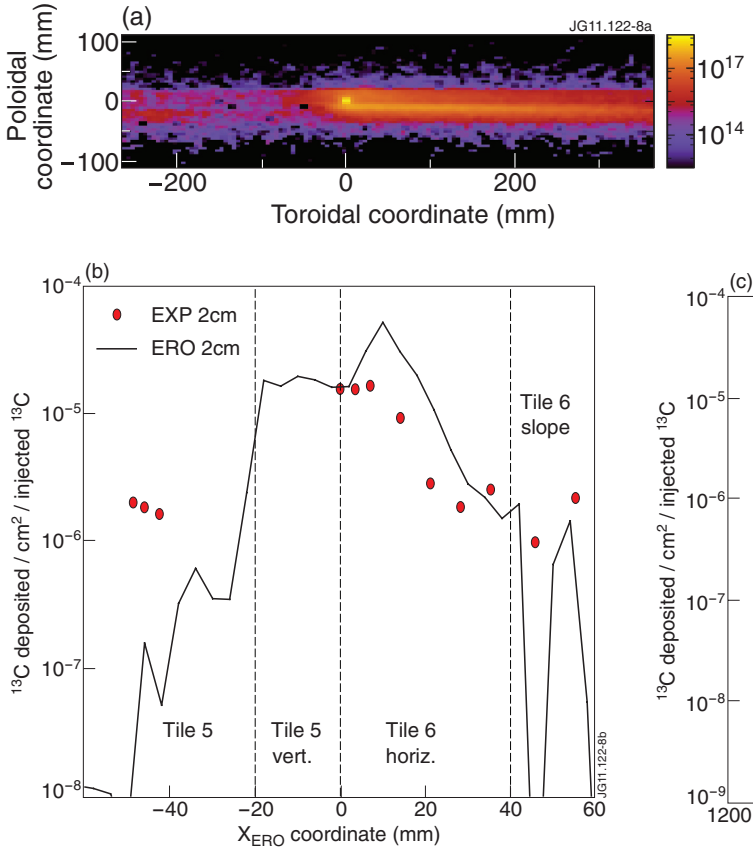

Figure 8: (a) Simulated 2D map for ^{13}C and (b) experimental and calculated poloidal distribution for ^{13}C, both experimental and calculated profile 2 cm from the puffing location, (c) ^{13}C deposition on Tile 7 simulated with ERO.